SEISMIC TOMOGRAPHY STUDY OF THE KAWERAU REGION AND WHAKATANE GRABEN (BAY OF PLENTY, NEW ZEALAND)

XIAOLI XIE[1] AND M.P. HOCHSTEIN [2]

[1] CRCAMET, Macquarie University, NSW 2109, Australia
[2] Geothermal Institute, The University of Auckland, NZ

SUMMARY: The crustal seismic velocity structure of the Kawerau geothermal field was investigated by a seismic tomography study using travel times of aftershocks associated with the 2 March, 1987 Edgecumbe earthquake. A total of 887 travel times from 89 events were used. Using the square of the slowness as a parameter to obtain continuous velocity-depth functions, inversion solutions were obtained using a damped least square algorithm to solve the large system of equations. The study shows that the Kawerau Field lies at the SW end of a crustal low velocity structure which extends from Kawerau to the north (over 30 km); the structure is well defined between 3 and 6 km depth. The seismic velocity anomaly occurs in brittle greywacke basement rocks beneath the tectonically very active Whakatane Graben. The low velocities probably reflect intense fracturing associated with active NNE trending faults. A low velocity anomaly also occurs beneath the E Kawerau field; however, it can not be separated from the much larger anomaly beneath the Graben.

1. INTRODUCTION

The epicentre of the Edgecumbe earthquake (2 March, 1987, M_L = 6.3) occurred c. 20 km NNW of the Kawerau Geothermal Field; the event was accompanied by more than 700 aftershocks of $M_L > 3$ during the period of 2. to 16.3.87 (Anderson et al., 1990). Temporary recording stations were installed soon after the main event and over 100 aftershocks could be located which occurred 3 to 9 days after the main shock (Robinson, 1989). The aftershock epicentres were confined mainly to the on-shore segment of the Whakatane Graben. A plot of the epicentres shows that there is a significant gap in seismicity in an area covered by the Kawerau Geothermal Field and the adjacent Mt. Edgecumbe Volcano, dormant in the last 3000 yrs (see Fig.1). The location of the Kawerau Field in Fig.1 was taken from Allis et al. (1993).

If one traces the rays between epicentres and stations surrounding the Kawerau Field, it can be seen that several rays must have travelled through the geothermal reservoir and through the substructure of Edgecumbe Volcano. An attempt was made to investigate the crustal velocity structure beneath both areas by using the seismic tomography method and observed travel times of well located aftershocks. The study was extended to cover the whole sector of the Whakatane Graben and was completed as a Geothermal Diploma Project (Xie, 1993).

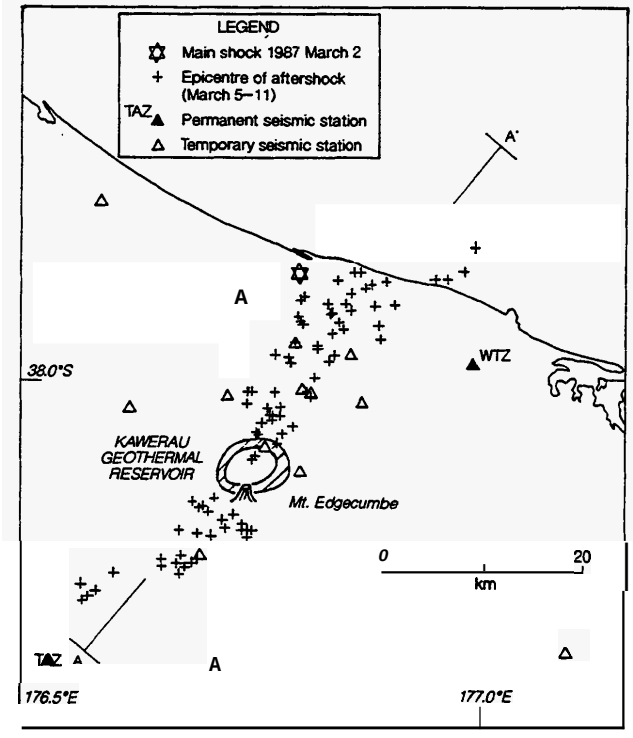

Fig.1 Map showing location of 89 aftershock epicentres selected for this study from the aftershock sequence of the 1987 Edgecumbe earthquake. Shown are also the location of temporary and permanent seismic stations.

2. STRUCTURE of GEOTHERMAL SYSTEMS and SEISMIC TOMOGRAPHY

Several studies have been made to elucidate the seismic velocity structure of geothermal systems and larger volcanic centres. The first successful study was that by Iyer (1975) who detected a pronounced seismic low velocity anomaly beneath the Yellowstone Caldera (USA) fiom observed time delays of teleseismic events. With suitable algorithms (for example, Aki and Lee, 1976), the observed velocity anomalies could be interpreted in terms of discrete velocity structures. Unfortunately, recording of teleseismic events is cumbersome and requires sophisticated networks.

Seismic tomography analysis was extended to analyse seismic refraction data using the 'time-term' method. In combination with 2-D and 3-D wave tracing methods, the velocity structure of discrete elements above the deepest refractor could be defined. The method was used, for example, by Lehman et al. (1982) to delineate the seismic velocity structure of the upper crust beneath Yellowstone Caldera (USA). A variation of the method was used by Henrys (1986) to analyse the 2-D velocity structure of the upper 200 m of the Ohaaki-Broadlands Field (NZ). The studies confirmed that P velocities decrease significantly in hot rocks and geothermal reservoirs; the effect is caused by complex changes of fluid properties and a decrease in matrix velocity with increasing temperature as found by laboratory studies (Nur, 1987).

Analysis of micro-earthquakes by the tomography method was more difficult since errors in observed travel times and resulting errors in hypocentres can cause ill- conditioned matrices during the inversion process. The problem was solved in part by introducing stabilizing criteria. The first tomography study of a large geothermal system, based mainly on micro-earthquake data, was that by Benz and Smith (1984) who studied the velocity structure of the huge Yellowstone system. In that study, blocks of large size were used (horizontal extent 21 x 18 km). It confirmed the results of the earlier studies by Iyer (1975) and Lehman et al. (1982) and showed that the velocity in upper crustal blocks was indeed up to 15% lower than that in blocks lying outside the large (60 x 50 km) caldera which contains at least four geothermal systems.

Meanwhile similar studies of smaller geothermal systems indicated that low velocity structures at greater depth can remain undetected if their lateral extent is small. Studies of the small (10 to 15 km ^{2}) Travale geothermal field in Italy by Hirn and Ferrucci (1985) showed, for example, that a significant P-wave time delay of teleseismic events could only be observed at a single station in the centre of the field. Time delays fiom local earthquakes and calibration shots showed an irregular pattern pointing to significant diffraction. This is probably caused by the so-called Wielandt effect (Nolet, 1987) which implies that the onset of positively delayed waves will be drowned by the arrival of diffracted waves and that smaller 'slow' regions may remain undetected. The effect also implies that a tomography model, containing both high and low velocity bodies, can be biased towards high velocity structures. This might explain the rather complex velocity structure beneath the Hengill geothermal system studied by Foulger and Toomey (1989) who used a rather small block size (2 x 2 km).

3. INPUT DATA and ORIGINAL VELOCITY STRUCTURE

The travel time data used for the tomography study of the Whakatane Graben consist of 887 P-wave travel times from 89 aftershocks whose epicentres are shown in Fig.1. The data are a subset of travel times of 112 events analysed by Robinson (1989). We selected only events for which the origin time was controlled by a clear S-phase observed at least at one station.

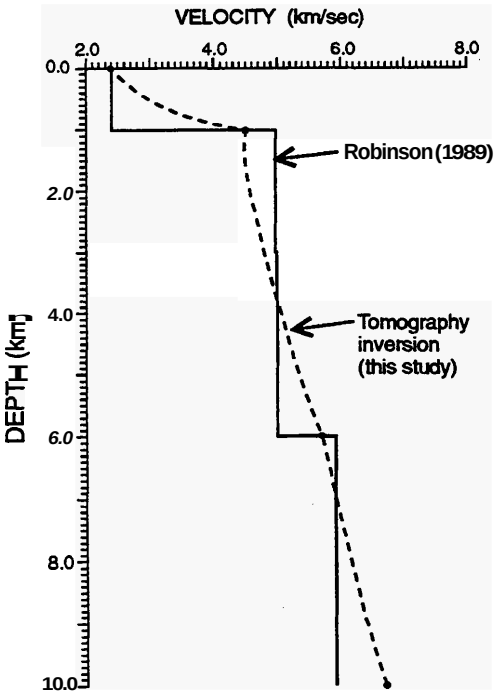

Fig.2 Approximate crustal velocity structure of the greater area surrounding the Whakatane Depression (model with solid lines from Robinson, 1989); the initial velocity model for the tomography study is shown by the dashed line.

A horizontal grid of 5 x 5 km was adopted; the model was extended to 10 km depth and each column was further subdivided by horizontal layers with subsurfaces at 1, 3, and 6 km depth. This subdivision reflects the gross regional velocity structure obtained by Robinson (1989) from the analysis of the aftershocks (see Fig.2). This velocity structure was further refined by introducing a non-linear changing velocity model as part of the tomography study assuming that the square of the slowness u of the seismic wave (u being the inverse of velocity v) varies linearly within each column (see dashed profile in Fig. 2).

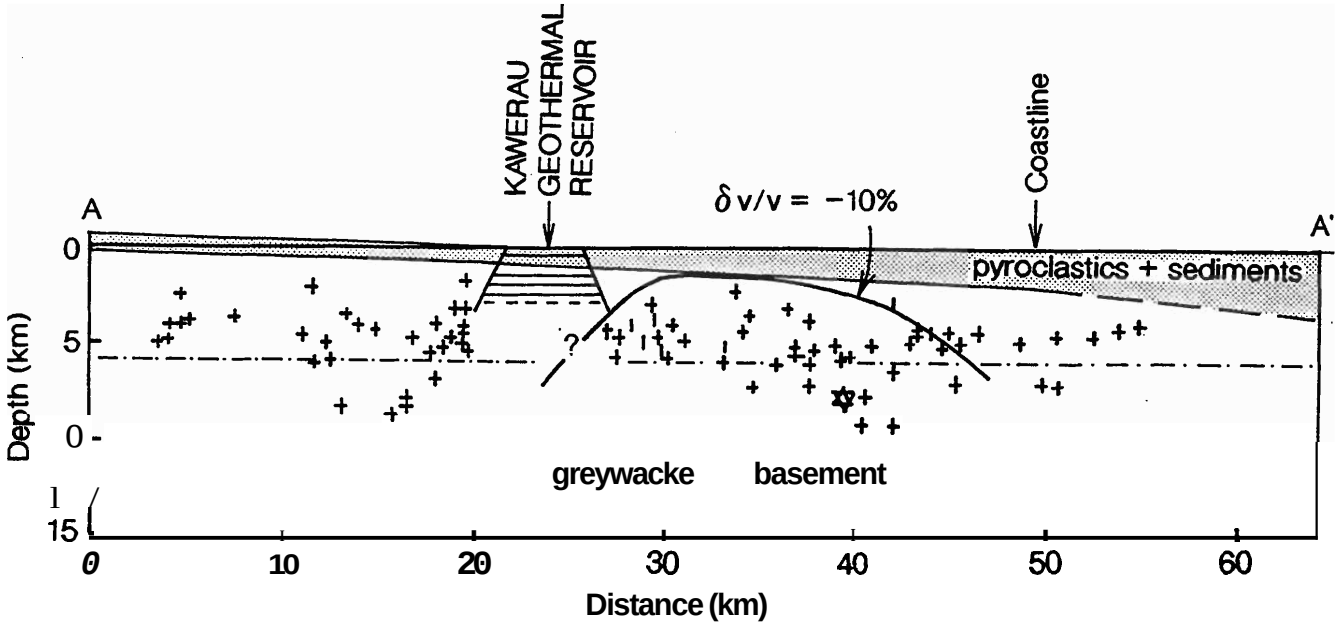

Fig.3 Vertical section showing location of the aftershock foci projected onto an axial profile AA' (for location see Fig. 1).

The actual velocity structure of the rocks in the area, however, differs significantly from that of a horizontally layered structure. The likely geological structure along an axial profile of the Whakatane Graben is shown in Fig.3. It can be seen that the thickness of layer 1, representing a layer of Quaternary pyroclastics and sediments, increases from less than 0.3 km at the southern end of the section (A) to c. 1.5 to 2 km at the seashore (A'). The figure also shows that most of the aftershock foci (projected onto section A A) occur in a rather narrow band between 3 and 6 km depth.

Lateral variations in the thickness of layer 1 are also indicated by the residual gravity anomalies shown in Fig. 4 where low density near-surface sediments show up with an elongate shaped negative gravity anomaly. The approximate thickness of layer 1 can be estimated from Fig.4. Velocity inhomogeneities are also reflected by the residual station times obtained by Robinson (1989) which show time delays of up to 0.2 sec at stations over the thick Quaternary infill and early arrivals of up to 0.27 sec at stations located over greywacke basement.

We reduced most of these effects by computing appropriate delay times assuming that most arrivals were associated with refracted waves. At first the "topographic delay" was assessed by reducing each travel time to a value as it would have been observed at sea level. In a second step the block of the fictitious layer 1 of the model in Fig. 2 was replaced by an equivalent layer reflecting the likely velocity structure of rocks beneath each station. The resulting corrections were usually within ± 0.1 sec of the residual station times of Robinson (1989) except for stations with station heights > 500 m.

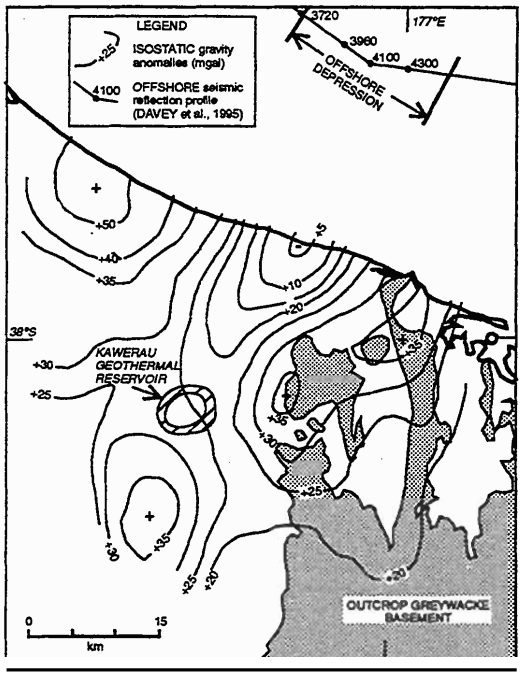

Fig.4 Map of isostatic gravity anomalies for the greater area surrounding the Whakatane Graben, the Graben can be recognized from the contour pattern.

4. METHOD

A non-linear seismic travel time tomography method was used which has been described by Cerviny (1987) and which has been modified and adapted by Song (1993). It leads to a linearization of the inversion by introducing the square of the slowness vector $u^2(x)$ as parameter. Assuming that the magnitude of $u^2(x)$ varies linearly within a given column segment, defined by the velocity v_i and v_{i+1} at top and bottom (nodes) respectively, the travel time of m seismic rays within a tomographic model containing n nodes (defining u) can be written in matrix form as:

$$[G]\,[q] = [t]\,, \qquad (1)$$

where $[G]$ is an m x n matrix,
$[q]$ is an n - D (square of slowness) vector whose transposed version
$[q]^T$ contains the whole velocity (square of slowness) structure $(q_1, q_2, \ldots q_n)$,
and $[t]$ is an m - D vector containing all observed travel times.

The evaluation of $[G]$ involves 3-D ray tracing applied to $u^2(x)$ as proposed by Virieux et al. (1988) and further modified by Song (1993). The solution of (1) is stabilized by introducing a damped least squares algorithm (Paige and Saunders, 1982; Bregman et al., 1989) using a damping factor h. Starting with an initial velocity (slowness) model denoted by, say, $[q_c]$, a better estimate $[q]$ can be obtained from:

$$[q - q_c] = [G^T G + h I]^{-1} G^T [t - G q_c] \qquad (2)$$

where I is an identity matrix.

5. TEST RESULTS

Preliminary analyses of the model were made to check whether the initial model would lead to an adequate resolution of deeper velocity anomalies. In addition, we had to check whether orientation and size of the grid could introduce a bias and whether the data set contained a few poor data which could produce pseudo-velocity anomalies.

Since the effective resolution of a tomography study is about 4 times that of the best possible resolution (of the order of 1/2 a wavelength for any wave in a given block), the selected grid size of 5 x 5 km was a bit greater than the optimum size for waves at 3 km depth with a peak frequency (observed) of 5 Hz. Further tests were made with a 4 x 4 and a 7 x 7 km grid which showed that the 5 x 5 km grid provided indeed better results. As for a possible bias caused by the grid orientation, we used initially a grid aligned 020°, i.e. the average strike of the Whakatane Graben. The major velocity anomaly was found to be aligned in that direction. Hence, we shifted the orientation to a N-S aligned grid which did not change significantly the pattern of the major velocity anomaly.

The rather coarse grid, however, led to abrupt changes of the velocity anomaly at its margins. The boundary structure was checked by shifting grid points by half a grid size (i.e. 2.5 km). Results were found to be spatially consistent.

A check for a possible bias caused by faulty travel time data involved a split into two sets of data which were randomly selected. The shape of the velocity anomaly pattern did not change. At the end of the tests we were satisfied that the results of the tomography study were not significantly affected by the choice of the initial model nor by faulty data.

6. DISCUSSION

Since the focal depth of most aftershocks was within the depth range of 3 to 6 km, this is also the depth range for which the velocity structure of the tomography model is best controlled. The seismic velocity of rocks at 3 and 6 km depth are shown in Fig.5 and Fig.6 respectively. It can be seen that at 3 km depth an elongate shaped low velocity structure occurs whose centre lies c. 5 km NE of the Kawerau Field. The anomaly extends for at least 30 km in NS direction and is c. 14 km wide. The average velocity of rocks at 3 km depth decreases from c. 5 km/s outside to 4.2 km/s inside (c. 16% decrease). The anomaly pattern at 6 km depth is rather similar to that at 3 km depth except that the anomaly axis has been shifted slightly towards NNE direction.

The surprising result of the study is that the suspected low velocity anomaly associated with hot crustal rocks beneath the Kawerau Geothermal Field and beneath Mt. Edgecumbe cannot clearly be recognised in Figs. 5 and 6 since it is concealed by a much larger N to NNE trending low velocity anomaly of regional extent. There exists, however, a low velocity anomaly beneath the eastern part of the Kawerau Field as found by our subgrid analysis.

The seismicity gap in the foci distribution (see Figs.1 and 3) also points to anomalously hot, and hence, ductile rocks beneath the Kawerau reservoir which do not sustain seismic 'stick slip'. Seismicity gaps beneath some high temperature reservoirs have been noticed in other seismically active regions, for example the Coso geothermal system in California (Combs and Rotstein, 1976); such a gap beneath Kawerau is therefore not an anomalous feature.

The widespread occurrence of aftershock foci outside the Kawerau Field points therefore to brittle crustal rocks which might be heated, but whose temperatures at, say, 3 km depth are significantly lower than those beneath the Kawerau Field (> 300°C). The low velocity anomaly cannot be interpreted in terms of anomalously high crustal temperatures in the depth range of 3 to 6 km.

Drill hole data from Kawerau and near Edgecumbe township, as well as seismic refraction data (Woodward, 1989) and residual gravity anomalies (see Fig.4) suggest that the Whakatane Graben is underlain by a coherent greywacke basement (Nairn and Beanland, 1989). The Graben continues to the NNE and widens offshore; the lateral extent of the structure is indicated in Fig.4, showing its location along an offshore reflection-refraction profile (Davey et al., 1995). Since the seismic low velocity anomaly covers most of the Graben on land which is dissected by parallel, generally NNE trending branches of the TVZ fault belt, we believe that the anomaly outlines a wide belt of intensely fractured basement rocks. A groundwater boron anomaly occurs downstream from the Kawerau

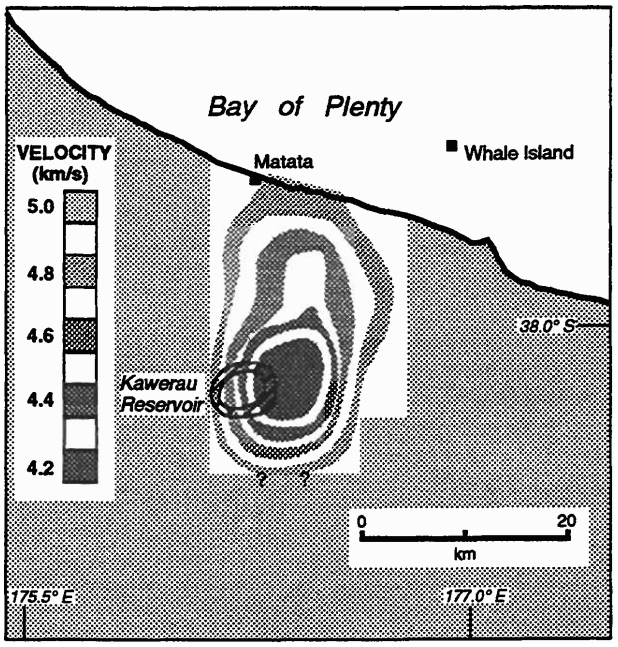

Fig.5 Seismic P-wave velocity of tomography model at a level of -3 km (velocity values computed for the centre (node) of single columns of size **5** x **5** km have been smoothed by contouring.

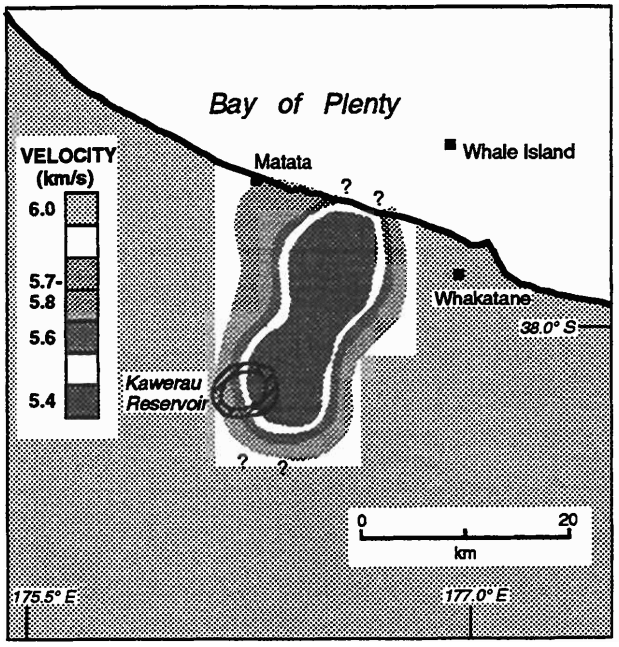

Fig.6 Seismic P-wave velocity of tomography model at a level of -6 km.

Geothermal Field (Allis et al, 1993). The anomaly lies above the crustal low velocity zone thus supporting the interpretation that the boron originates from a deeper, northward directed outflow of mixed thermal waters in fractured basement rocks.

Crustal low velocity anomalies associated with wide fracture zones have been found elsewhere by tomography studies. A crustal low velocity anomaly is for example associated with a NNW trending fracture zone which runs close to the Mount St. Helens Volcano (Lees and Crosson, 1989); the anomaly has a lateral extent which is similar to that shown in Figs.5 and 6, although the margins are less well defined. A low velocity anomaly at 3 km depth also occurrs at the W margin of the San Andreas fault belt near Parkfield (California) and was found by a tomography study (Lees and Martin, 1990). There are therefore examples which show that certain segments of large fault belts are associated with low velocity crustal rocks and that the lateral extent of these anomalies can be similar to that of the low velocity belt beneath the Whakatane Graben. The overall decrease in seismic P-wave velocity in the examples cited is similar to that shown in Figs. **5** and 6.

Our study has led to the discovery of a large seismic velocity anomaly beneath the Whakatane Graben which can be interpreted in terms of a concealed crustal fracture zone. The zone, here called the 'Whakatane Graben fracture zone', is the result of continous tectonic deformations associated with the oblique opening of the whole Taupo Volcanic Zone.

The Kawerau geothermal reservoir lies at the SW margin of the Whakatane Graben low velocity anomaly. The model used in our study had insufficient resolution to outline the Kawerau structure in more detail.

7. REFERENCES

Aki, K., Lee, W.H.K. (1976). Determination of three-dimensional velocity anomalies under a seismic array using first P arrival times from local earthquakes. Part I. A homogeneous initial model. Journ. Geophysical Res. 81,4381 - 4399.

Allis, R.G., Christensen, B.W., Nairn, I.A., Risk, G.F., White, S.P. (1993). The natural state of Kawerau Geothermal Field. Proc. 15th NZ Geothermal Workshop, Univ. of Auckland, 227-233.

Anderson, H., Smith, E., Robinson, R. (1990). Normal faulting in a back arc basin: Seismological characteristics of the March 2, 1987, Edgecumbe, New Zealand, Earthquake. Journ. Geophysical Res. 95,4709 - 4723.

Benz, H.M., Smith, R.B. (1984). Simultaneous inversion for lateral velocity variations and hypocentres in the Yellowstone Region using earthquake and refraction data. Journ. Geophysical Res. 89, 1208 - 1220.

Bregman, N.D., Bailey, R.C., Chapman, C.H. **(1989).** Crosshole seismic tomography. Geophysics **54. 200 - 215.**

Cerveny, V. **(1987).** Ray tracing algorithms in three-dimensional laterally varying layered structures. In: Guust Nolet (Ed.) Seismic Tomography. D. Reidel Publishing Co., Dordrecht, **99 - 133.**

Combs, J., Rotstein, **Y. (1976).** Microearthquake studies at the Coso geothermal area, China Lake, California, Proc. 2nd UN Symp. on the Development and Use of Geothermal Resources, V01.2, **909 - 916.**

Davey, F.J., Henrys, S.A., Lodolo, E. **(1995).** Asymmetric rifting in a continental back-arc environment, North Island, New Zealand. Journ. Volcanology Geotherm. Res. **68,209 - 238.**

Foulger, G.R., Toomey, D.R. **(1989).** Structure and evolution of the Hengill - Grensdalur volcanic complex, Iceland: Geology, geophysics, and seismic tomography. Journ. Geophysical Res. **94, 17511 - 17527.**

Henrys, S.A. **(1986).** Shallow structure of the Broadlands - Ohaaki geothermal field (NZ): Analysis of seismic refracted arrivals by iterative ray tracing. Proc. 8th NZ Geothermal Workshop, Univ. of Auckland, **85 - 90.**

Hirn, A., Ferrucci, F. **(1985).** P and **S** arrival time anomalies at a dense array: marker of the Travale Field. Geothermics **14,713 - 727.**

Iyer, H.H. **(1975).** Anomalous delays of teleseismic P-waves in Yellowstone National Park. Nature **253, 425 - 427.**

Lees, J.M., Crosson, R.S. **(1989).** Tomography inversion for three-dimensional velocity structure at Mount St. Helens using earthquake data. Journ. Geophysical Res. **94,5716 - 5728.**

Lees, J.M., Malin, P.E. **(1990).** Tomographic image of P-wave velocity variation at Parkfield, California. Journ. Geophysical Res. **95, 21793 - 21804.**

Lehman, J.A., Smith, R.B., Schilly, M.M., Braile, L.W. **(1982).** Upper- crustal structure of Yellow-stone from seismic and gravity observations. Journ. Geophysical Res. **87, 2713 - 2730.**

Nairn, I.A., Beanland, S. **(1989).** Geological setting of the **1987** Edgecumbe earthquake, New Zealand. NZ Journ. Geology Geophys. **32, 1 - 13.**

Nolet, G. **(1987).** Seismic wave propagation and seismic tomography. In: Guust Nolet (Ed.) Seismic Tomography. D. Reidel Publishing Co., Dordrecht, 1 - **22.**

Nur, A. **(1987).** Seismic rock properties for reservoir description and monitoring. In: Guust Nolet (Ed.) Seismic Tomography. D. Reidel Publishing Co., Dordrecht, **203-237.**

Paige, C.C., Saunders, M.A. **(1982).** LSQR: An algorithm for sparse linear equations and sparse least squares. ACM Trans. Math. Softw.8, 43 - **71.**

Robinson, R. **(1989).** Aftershocks of the **1987** Edgecumbe earthquake, New Zealand: seismological and structural studies using portable seismographs in the epicentre region. NZ Journ. Geology Geophys. **32, 61 - 72.**

Song L. **(1993).** Ray tracing of the square of slowness and non-linear seismic travel time tomography. Journ. Chengdu College of Geology **20** (No. **1),** (in Chinese).

Woodward, D.J. **(1989).** Geological structure of the Rangitaiki Plains near Edgecumbe, New Zealand, from seismic data (Note). NZ Journ. Geology Geophys. **32, 15 - 16.**

Virieux, J., Farra, V., Madriaga, R. **(1988).** Ray tracing for earthquake location in laterally heterogeneous media. Journ. Geophysical Res. **93,** 6585-6599.

Xie, Xiaoli **(1993).** Seismic tomography study of onshore Whakatane Graben. Unpubl. Geothermal Dipl. Report **93.26,** lodged in Library, Univ. of Auckland.